New anticancer active and selective phenylene-bisbenzothiazoles: Synthesis, antiproliferative evaluation and DNA binding

ARTICLE *in* EUROPEAN JOURNAL OF MEDICINAL CHEMISTRY · MARCH 2013

Impact Factor: 3.45 · DOI: 10.1016/j.ejmech.2013.02.026 · Source: PubMed

European Journal of Medicinal Chemistry 63 (2013) 882–891

Contents lists available at SciVerse ScienceDirect

European Journal of Medicinal Chemistry

journal homepage: http://www.elsevier.com/locate/ejmech

Original article

New anticancer active and selective phenylene-bisbenzothiazoles: Synthesis, antiproliferative evaluation and DNA binding

Livio Racané [a], Sandra Kraljević Pavelić [b], Raja Nhili [c], Sabine Depauw [c], Charles Paul-Constant [c], Ivana Ratkaj [b], Marie-Hélène David-Cordonnier [c,**], Krešimir Pavelić [b], Vesna Tralić-Kulenović [a], Grace Karminski-Zamola [d,*]

[a] Department of Applied Chemistry, Faculty of Textile Technology, University of Zagreb, baruna Filipovića 28a, 10000 Zagreb, Croatia
[b] Division of Biotechnology, University of Rijeka, Radmile Matejčić 2, 51000 Rijeka, Croatia
[c] INSERM U837-JPARC (Jean-Pierre Aubert Research Center), Team Molecular and Cellular Targeting for Cancer Treatment, Université Lille Nord de France, IFR-114, Institut pour la Recherche sur le Cancer de Lille, Place de Verdun, F-59045 Lille Cedex, France
[d] Department of Organic Chemistry, Faculty of Chemical Engineering and Technology, University of Zagreb, Marulićev trg 20, P.O. Box 177, HR-10000 Zagreb, Croatia

ARTICLE INFO

Article history:
Received 31 January 2013
Received in revised form
21 February 2013
Accepted 22 February 2013
Available online 14 March 2013

Keywords:
Amdino-substituted phenylene-bisbenzothiazoles
Antitumour evaluation
DNA-binding
Apoptosis

ABSTRACT

Novel amidino-derivatives of phenylene-bisbenzothiazoles were synthesized and tested for their antiproliferative activity against several human cancer cell lines, as well as DNA-binding properties. The synthetic approach used for preparation of isomeric amidino substituted-phenylene-bis-benzothyazoles **3a**–**3f** was achieved by condensation reaction of isophthaloyl dichloride **1a** and terephthaloyl dichloride **1b** or with phthalic acid **1c** with 5-amidinium-2-aminobenzothiolate **2a** and 5-(imidazolinium-2-yl)-2-aminobenzothiolate **2b** in good yields. The targeted compounds were converted in the desired water soluble dihydrochloride salts by reaction of appropriate free base with concd HCl in ethanol or acetic acid. All tested compounds (**3a**–**3f**) showed antiproliferative effects on tumour cells in a concentration-dependant manner. The strongest activity and cytotoxicity was observed for diimidazolinyl substituted phenylene-bisbenzothiazole compound **3b**. These effects were shown to be related to DNA-binding properties, topoisomerase I and II poisoning effects and apoptosis induction. The highest tested selectivity towards tumour cells was observed for the imidazolyl substituted phenylene-benzothiazole **3d** that showed no cytotoxic effects on normal fibroblasts making it an excellent candidate for further chemical optimization and preclinical evaluation.

1. Introduction

Despite major breakthroughs in many areas of modern medicine over the past 50 years, the relative mortality rate caused by cancer is still very high. Indeed, cancer accounts for more than 20% of all deaths. Early diagnosis and prevention are still the most effective tools against cancer disease whose incidence and mortality rates are highly increased during the last decades in developed countries. Classical chemotherapy, using small molecules or bioactive natural products is still the mainstay for cancer treatment that is directed towards inhibition of cellular targets such as DNA, tubulin, or protein kinases [1–3]. The use of available chemotherapeutics is however, rather limited due to severe side effects or a limited choice of available anticancer drugs. This clearly underscores the rationale for development of more effective cancer treatments and new class of chemotherapeutics.

Benzothiazole derivatives are of considerable interest due to diverse pharmaceutical properties and were studied extensively for their antimicrobial [4–6], antitumour [7–10], and antiviral [11,12] activities. Interesting data has also been reported for this class of compounds regarding anti-HIV properties [13] and inhibition of kinases [14]. 2-Arylbenzothiazoles emerged as a privileged scaffold in drug discovery bearing remarkable activity profiles in non-invasive diagnosis of Alzheimer's disease and antitumour effects [15]. Tasler et al. described the synthesis of corresponding aminophenyl-substituted benzothiazoles with different adenine mimic and described the identification of promising scaffolds that are able to inhibit different kinases with the IC_{50} values in the nanomolar range

* Corresponding author. Tel.: + 385 14597215; fax: +385 14597250.
** Corresponding author. Tel.: +33 320169223; fax: +33 320169229.
E-mail addresses: marie-helene.david@inserm.fr (M.-H. David-Cordonnier), gzamola@fkit.hr (G. Karminski-Zamola).

0223-5234/$ – see front matter © 2013 Elsevier Masson SAS. All rights reserved.
http://dx.doi.org/10.1016/j.ejmech.2013.02.026

[16]. Besides the benzothiazole core and its numerous potential biological implications, the central rings and attached substituents play a major role in the binding affinity and selectivity. Indeed, for the particular case of DNA binding of benzothiazole derivatives, engrafting amidines extremities to those structure, as positively charged substituents, orientate the function of the molecule towards the binding to electronegatively charged biological molecule such as DNA in a similar manner than berenil, pentamidine, stilbamidine, furamidine and other diamidine heterocycles [17,18].

Our previously published data showed accentuated antiproliferative effects for this class of compounds as well. We found that antiproliferative activity of amidino- [19,20] and amino- [21] substituted 2-phenylbenzothiazole derivatives strongly depend on the position of the substituent on 2-phenylbenzothiazole skeleton, as well as on the type of attached amidino substituent. We found that, in a series of unsubstituted, *N*-isopropyl substituted, as well as 2-imidazolinyl mono- and diamidino derivatives of 2-phenylbenzothiazole, *N*-isopropyl substituted amidine possess less pronounced antiproliferative activity on tested tumour cell lines.

In relation with the above considerations and as a continuation of our recent encouraging results [22], we synthesized new diimidamidyl, and diimidazolinyl substituted phenylene-bisbenzo thiazoles and evaluated their antiproliferative activity on tumour cell lines *in vitro*, DNA binding propensity, sequence-selectivity as well as topoisomerases inhibition. Two compounds were chosen according to their potency and differential effect on tumour cell lines for further biological studies including the cell cycle analysis and apoptosis induction in order to reveal a more detailed picture on the possible antiproliferative mechanisms and/or targets.

2. Results and discussion

2.1. Chemistry

The synthesis of phenylene diamidino-substituted bisbenzothiazole derivatives **3a**–**3f** was performed by condensation reactions according to Scheme 1.

Amidino-substituted *o*-aminothiophenole **2a** and **2b** were the key precursors for the synthesis of bisbenzothiazole derivatives which was recently developed as a convenient method for their synthesis [23]. This allowed us to use classical synthetic approach for the synthesis of 2-substitited benzothiazoles by condensation reaction of *o*-aminothiophenoles with aldehydes, carboxylic acids, acyl chlorides, or esters. We found [19,22] that condensation of amidino-substituted *o*-aminothiophenoles with acyl chlorides in glacial acetic acid is the most convenient condensation reaction giving the corresponding 2-substituted benzothiazolyl compounds in high yields. Thus, condensations of commercially available isophthaloyl dichloride **1a** and terephthaloyl dichloride **1b** with 5-amidinium-2-aminobenzothiolate **2a** and 5-(imidazolinium-2-yl)-2-aminobenzothiolate **2b** gave the corresponding targeted compounds **3a**–**3e** which were isolated as dihydrochloride salts in excellent yield of about 90%. In spite of this condensation method, great number of commercially available carboxylic acids prompted us to optimize reaction for their condensation with *o*-aminothiophenoles in polyphosphoric acid (PPA) because the usual condensation reaction at 180 °C throughout 2–3 h gives product in low to moderate yield. Gradually heating the mixture of phthalic acid **1c** with amidino-substituted *o*-aminothiophenole **2a**

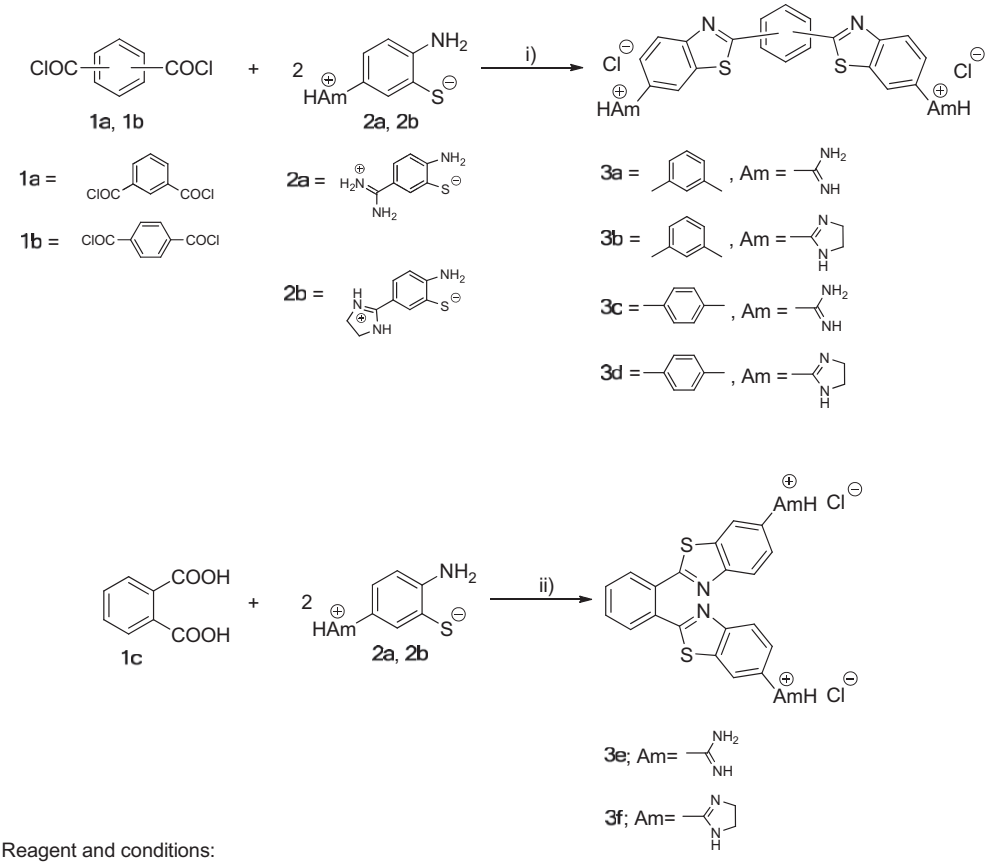

Scheme 1.

and **2b** were performed by heating the mixture at 120–140 °C for the first 1 h at 120–140 °C, and then at 160–180 °C for additional 2 h significantly improved the yield of the condensation products and after conversion of the corresponding free base into dihydrochloride salts gave pure products **3e** and **3f** in a good yield of about 65%. The structure of compounds **3a**–**3f** was determined by ^{1}H and ^{13}C NMR spectroscopy, MS spectrometry, as well as elemental analyses. Elemental analyses have shown that the corresponding dihydrochlorides were crystallised as tri hydrates.

2.2. Antitumour activity

The antiproliferative effect of novel phenylene-bisbenzothiazoles was evaluated on a panel of tumour cell lines *in vitro* and normal human fibroblasts (WI38). All tested compounds demonstrated antiproliferative effect in a concentration-dependant manner on majority of tested cell lines (Table 1). These results are in complete agreement with our previous studies [24] and published literature data [25,26]. The strongest antiproliferative effect and a high cytotoxicity (Table 2) was exhibited by compound **3b**, which successfully inhibited the growth of tested cell lines at submicromolar concentrations (1 and 0.1 μM). Compound **3d** showed a strong selectivity towards tumour cell lines at submicromolar concentrations (1 and 0.1 μM) and no cytotoxic effect on normal human fibroblasts. The weakest antiprofilerative effect was measured for compound **3f** that inhibited the growth of tumour cell lines only at highest tested concentrations (100 and 10 μM). Due to high selectivity of compound **3d** for tumour cell lines, it was chosen for further mechanistic studies. Compound **3b** was also evaluated for the biological effect due to the strongest antiproliferative effect observed on all tested cell lines.

2.3. Cell cycle analysis and Annexin V assay

Treatment of cells with compounds **3b** and **3d** induced strong cell cycle perturbations (Table 3). Compound **3b** induced an increase of SW620 cells in the S-phase and a concomitant decrease in the G2/M phase after 24 h at its lower concentration (5 μM). Similar results were observed for compound **3b** (at 10 μM) where the number of cells arrested in the S-phase was doubled in comparison with control along with an increase of apoptotic cells in the subG1 that is indicative of apoptosis. Prolonged treatment (48 h) of SW620 cells with compound **3b** maintained the S-phase arrest and increased the subG1 cell population. Induction of apoptosis by compound **3b** was confirmed by Annexin V assay. Indeed, compound **3b** at 10 μM effectively induced apoptosis after 48-h treatment in 95% of SW620 cells (Table 4). The effect of compound **3b** on the SK-BR-3 cell cycle was however, different: 24 h incubation with both tested concentrations induced an increase of cells in the subG1

Table 1
Antiproliferative effects of compounds **3a**–**3f** on the growth of tumour cells *in vitro*.

Substance	IC_{50}[a] (μM) Cell lines					
	MCF-7	SK-BR-3	SW620	MiaPaCa-2	WI38	HeLa
3a	5.34	83.2	6.01	>100	0.99	>100
3b	>100	0.04	0.47	0.26	0.15	2.06
3c	9.01	8.55	>100	20.4	41.93	9.6
3d	3.07	1.18	7.65	3.54	>100	7.75
3e	30.9	86.6	>100	44.8	86.4	63.6
3f	10.14	1.86	24.7	14.6	8.99	26.8

[a] IC50; 50% inhibitory concentration, or compound concentration required to inhibit tumour cell proliferation by 50%. The IC50 values were calculated from – concentration – response curves using linear regression analysis by fitting the mean test concentrations that give PG values above and below the reference value.

Table 2
Cytotoxic effects of compounds **3a**–**3f** on the growth of tumour cells *in vitro*. The results are presented as LC50 values in μM. The cell growth rate was evaluated by the MTT assay: experimentally determined absorbance values were transformed into a cell percentage growth (PG) using the formulas proposed by National Cancer Institute and described previously in Gazivoda et al. [27].

Substance	LC_{50}[a] (μM) Cell lines					
	MCF-7	SK-BR-3	SW620	MiaPaCa-2	WI38	HeLa
3a	>100	>100	>100	>100	65.4	>100
3b	5.3	0.87	6.19	1.49	6.63	7.38
3c	>100	>100	>100	>100	>100	>100
3d	>100	8.07	>100	36.7	>100	71.1
3e	>100	>100	>100	>100	>100	>100
3f	71.4	67.9	81.3	72.9	74.3	76.4

[a] LC_{50}; 50% inhibitory concentration, or compound concentration required to inhibit tumour cell proliferation by 50% in comparison with the cell number at day 0.

accompanied with a decrease of cells in the G1 phase. Interestingly, higher concentration of **3b** increased the percentage of cells in the G2/M phase while lower concentration induced the opposite effect. A similar pattern has been observed upon 48-h treatment of SK-BR-3 cells with compound **3b**. Apoptosis was again confirmed as 75% of SK-BR-3 cells treated with compound **3b** at 10 μM were in late apoptosis after 48 h treatment (Table 4). Treatment of MiaPaCa-2 cells with compound **3b** at 5 μM increased the G1 and subG1 cell populations after 24 h while higher concentration induced a decrease of cells in G1 and subG1 phases accompanied with an increase of cells in the S-phase after 48 h. A marked increase of cells in the S-phase has been observed in HeLa cells as well upon treatment with **3b** in a concentration-dependant manner after 24 h and a decrease in G1 and G2/M phases after 48 h treatment with both concentrations.

Significant cell cycle perturbations were observed for compound **3d** as well. In MiaPaCa-2 cells lower concentration (5 μM) increased the subG1 and S-cell populations after 24-h treatment and a concomitant decrease of cells in the G2/M phase. Moreover, higher concentration (10 μM) induced a substantial rise of subG1 cell population after 24 and 48 h (Table 3). Interestingly, Annexin V assay did not confirm induction of apoptosis (Table 4) pointing to another mechanism of cell death. Compound **3d** exerted a weak effect on the SK-BR-3 cell cycle after 24 h (rise of cell percentage in the subG1 phase at higher tested concentration). However, after 48 h treatment an increase of cells in the subG1, G1 and G2/M phases followed by a decrease of cells in the S phase has been observed. Results of Annexin V assay confirmed induction of apoptosis in SK-BR-3 cells (Table 4). In HeLa cells compound **3d** decreased the percentage of cells in the G1 and G2/M phases after 24 h with a concomitant increase of cells in the S-phase that persisted after 48 h as well at higher tested concentration.

2.4. DNA binding potency and mode of DNA interaction

Compounds **3a** to **3f** were then evaluated for DNA binding propensity. At a first sight, the variation of drug absorbency upon addition of the DNA was evaluated using UV/visible spectrometry (Fig. 1). Even at low concentration of CT-DNA, hypochromic effect was observed using all 6 compounds. This was followed by a hyperchromic effect for compounds **3a** and **3d**, together with a bathochromic effect particularly strong for compound **3d**. In the latter, a transition is observed but with a lost of the isosbestic point at intermediate CT-DNA concentrations suggestion a transition associated with a different binding mode. A clear isosbestic point was seen for compounds **3e** and **3f** suggesting a single mode of binding with those.

Table 3
Flow cytometric analysis of the cell cycle upon 24- and 48 h- treatments of SW620, MiaPaCa-2, SK-BR-3 and HeLa with compound **3b** and MiaPaCa-2, SK-BR-3 and HeLa treatment with compound **3d** at concentrations 5 and 10 μM. Cells were stained with propidium iodide and analysed with Becton Dickinson FACScalibur flow cytometer (10,000 counts were measured for each condition). The percentage of the cells in each cell cycle phase is based on the obtained DNA histograms and was determined by WinMDI 2.9 and Cylchred software. The results are presented as cell percentages (%).

Cell line/treatment	Cell percentage (% ± standard deviation)			
Compound **3b**				
SW620	subG1	G1	S	G2/M
Control-24 h	16 ± 1.4	43.7 ± 7	27.9 ± 2.9	24 ± 1.4
5 μM-24 h	13.5 ± 0.9	45.3 ± 3.2	**46.6 ± 1.4**[a]	**15.5 ± 0.7**[a]
10 μM −24 h	**45.3 ± 3.2**[a]	29.9 ± 0.2	**65.6 ± 3.1**[a]	23.9 ± 1.5
Control-48 h	2.3 ± 0.3	33.3 ± 2.4	44 ± 10.3	17.6 ± 0.6
5 μM-48 h	**24.8 ± 4.3**[a]	36.7 ± 7.5	48.6 ± 3.2	14.7 ± 4.4
10 μM-48 h	**13.6 ± 2.8**[a]	**23.7 ± 1.6**[a]	**69.6 ± 2.6**[a]	6.8 ± 4.1
SK-BR-3				
Control-24 h	14.6 ± 0.9	61.9 ± 2.5	51.9 ± 2.7	8.7 ± 0.4
5 μM-24 h	**33.3 ± 3.9**[a]	**34.5 ± 1.8**[a]	58.9 ± 5.3	**4.2 ± 0.1**[a]
10 μM-24 h	**23.1 ± 2.4**[a]	**28.7 ± 2.5**[a]	62.1 ± 4.9	**17.8 ± 0.6**[a]
Control-48 h	12.3 ± 1.5	49.4 ± 5.9	35.8 ± 3.9	14.8 ± 1.9
5 μM-48 h	**21.6 ± 0.8**[a]	36.2 ± 2.1	44 ± 1.3	21.1 ± 1.6
10 μM-48 h	12.5 ± 2.9	**22.1 ± 2.6**[a]	67.8 ± 0.1	11.1 ± 1.5
MiaPaCa-2				
Control-24 h	10.9 ± 0.9	43.7 ± 4.9	50.1 ± 4.7	15.1 ± 2.5
5 μM-24 h	**17.7 ± 0.3**[a]	**60.2 ± 1.7**[a]	33.6 ± 5.9	10.9 ± 2.3
10 μM −24 h	8.1 ± 0.7	41.6 ± 2.2	49.1 ± 6.3	21.3 ± 0.6
Control-48 h	26.5 ± 6.4	47.1 ± 1.2	38.1 ± 0.4	14.9 ± 0.7
5 μM-48 h	20.4 ± 7.5	52.1 ± 2.7	30.8 ± 2.9	17.1 ± 0.2
10 μM-48 h	**9.1 ± 0.9**[a]	**42.8 ± 0.6**[a]	**50.8 ± 4.5**[a]	8.6 ± 0.8
HeLa				
Control-24 h	16.9 ± 2.4	41 ± 9.7	37.3 ± 0.8	21.6 ± 8.9
5 μM-24 h	14.4 ± 0.2	39.3 ± 2.4	**38.4 ± 0.3**[a]	24 ± 0.4
10 μM-24 h	12.5 ± 0.4	31.7 ± 0.2	**66.3 ± 1.1**[a]	2.1 ± 0.9
Control-48 h	17.3 ± 3.6	52.8 ± 2.5	63.9 ± 5.6	21.5 ± 2.2
5 μM-48 h	13.3 ± 1.3	**47.5 ± 6.8**[a]	39.3 ± 7.5	**17.2 ± 1.7**[a]
10 μM-48 h	15.5 ± 6.3	**20.4 ± 4.9**[a]	71.4 ± 3.6	**13.2 ± 1.6**[a]
Compound **3d**				
SK-BR-3				
Control-24 h	10.3 ± 1.9	49.8 ± 9.8	40.5 ± 5.1	12.1 ± 1.6
5 μM-24 h	15.8 ± 2.1	58.9 ± 3.5	33.5 ± 2.3	11.6 ± 0.1
10 μM-24 h	**31.6 ± 0.9**[a]	50.9 ± 2.5	39.1 ± 3.8	14.5 ± 0.2
Control-48 h	10.1 ± 1.4	29.3 ± 1.6	64.4 ± 4.0	7.1 ± 1.5
5 μM-48 h	**27.5 ± 0.3**[a]	**53.6 ± 0.2**[a]	**32.6 ± 0.2**[a]	**13.8 ± 0.3**[a]
10 μM −48 h	**32.1 ± 3.7**[a]	**41.3 ± 0.9**[a]	42.3 ± 9.8	**20.3 ± 3.3**[a]
MiaPaCa-2				
Control-24 h	21.2 ± 0.5	50.4 ± 6.1	36.8 ± 3.9	20.3 ± 0.6
5 μM-24 h	**34.4 ± 0.4**[a]	35.2 ± 2.2	**55 ± 2.3**[a]	**5.8 ± 0.2**[a]
10 μM-24 h	**33.1 ± 0.3**[a]	40.9 ± 1.1	40.1 ± 4.1	19 ± 5.2
Control-48 h	29.1 ± 2.4	45.8 ± 5.1	38.6 ± 2.5	20.6 ± 4.6
5 μM-48 h	35.7 ± 5.7	45.9 ± 3.5	35.8 ± 2.4	18.4 ± 1.1
10 μM −48 h	**53.9 ± 1.1**[a]	40.6 ± 9.4	40.9 ± 9.8	18.4 ± 0.4
HeLa				
Control-24 h	12.1 ± 2.8	45.6 ± 1.7	41.1 ± 5.7	16.8 ± 2.5
5 μM-24 h	9.9 ± 0.2	42.0 ± 0.1	44.5 ± 0.2	13.4 ± 0.2
10 μM −24 h	15.5 ± 4.3	**34.2 ± 1.3**[a]	**58.7 ± 1.8**[a]	**7.2 ± 3.2**[a]
Control-48 h	14.4 ± 1.9	45.9 ± 5.5	34.6 ± 3.7	19.5 ± 0.7
5 μM-48 h	22.7 ± 3.9	31.9 ± 2.7	**49.6 ± 2.2**[a]	18.9 ± 1.3
10 μM-48 h	23.2 ± 2.5	42.3 ± 4.1	**44.0 ± 2.8**[a]	14.5 ± 3.1

[a] Statistically significant result: statistical analysis was performed in Microsoft Excel by using ANOVA at $p < 0.05$.

Based on observed DNA binding propensity, the compounds were evaluated by using double-strand DNA melting temperature studies to get an insight in the relative strength of the binding. Binding to CT-DNA was evaluated at drug/DNA ratio of 0.5 or 0.25 when 0.5 could not be used due to interference of the drug absorbency at such ration that impeded proper measurements. Compounds **3a**, **3b** and **3f** present the highest DNA binding propensity with Δ*T*m values greater than 10 °C (Table 5).

Table 4
Results of the Annexin V assay performed upon 24 and 48 h treatments of SW620 and SK-BR-3 with compound **3b** and MiaPaCa-2 and SKBR-3 with compound **3d**. The results are presented as percentages of cells positive to annexin and/or propidium iodide (apoptotic cells) per total counted cell number.

	Compound **3b**		Compound **3d**	
	SW620%	SK-BR-3%	MiaPaCa-2	SK-BR-3%
Control-24 h	7	8	5	6
10 μM-24 h	8	8	5	5
Control-48 h	10	19	3	5
10 μM-48 h	95	75	4	15

We then investigated the DNA binding mode for each compound. First we used circular dichroism spectrometry to differentiate groove binding to intercalation as modes of DNA interaction (Fig. 2). A large positive induced circular dichroism (ICD) was evidenced for compounds **3e** and **3b** suggesting (minor) groove binding. A weaker positive ICD was obtained for compounds **3f** and **3a** suggesting less efficient groove binding for those compounds. By contrast, no changes in the CD spectra were observed for the para-substituted compounds **3c** and **3d**.

Because of the strong groove binding properties of compound **3b** and **3e** evidenced during ICD measurements, compounds from this series were further evaluated for their sequence-selective binding by use of DNase I footprinting assays. Only **3b** evidenced some sequence selectivity as exemplified by the sites protected from nuclease activity localised using grey boxes. These protected portions of DNA correspond to AT-rich sites.

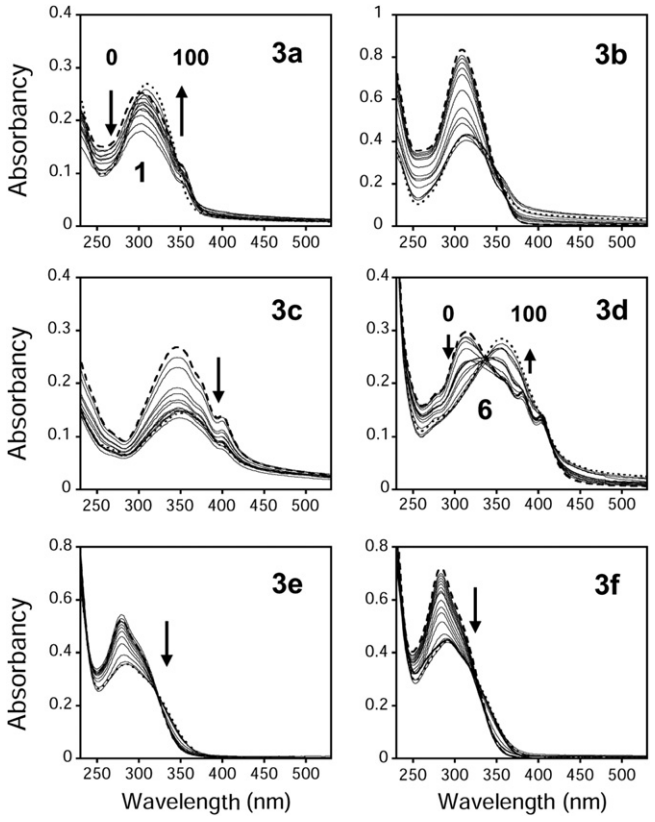

Fig. 1. UV/Vis spectra analyses of the drug/DNA interaction. 20 μM of each compound was incubated alone (bold dashed lanes) or with a step by step increase of CT-DNA concentrations from 0.1 to 100 μM (bold dotted lanes). The spectra were recorded from 230 to 530 nm relatively to a reference cuvette containing the same amount of CT-DNA. Hypochromic and hyperchromic effects are exemplified using down and up arrows, respectively, with the concentration of compound at transition indicated a the bottom of the lanes (μM).

Table 5
Variation of the melting temperature of CT-DNA upon binding of compounds **3a**–**3f** at the indicated drug/DNA ratio.

Compound	**3a**[a]	**3b**[a]	**3c**[b]	**3d**[a]	**3e**[b]	**3f**[b]
Δ*T*m (°C)	13.7	12.8	3	3.9	9.8	16.8

[a] drug/bp ratio = 0.25.
[b] drug/bp ratio = 0.5.

The compounds were further evaluated for their DNA intercalation properties by use of topoisomerase I-induced DNA relaxation assays (Fig. 4). Because of strong binding to the plasmid DNA, compounds **3a** to **3d** evidenced smearing of each plasmid forms (supercoiled, relaxed or linear) as part of a strong non-intercalating binding. This is in contrasts with the DNA forms obtained with the *ortho*-substituted compounds (**3f** and **3e**). Interestingly, compound **3f** is the only one than evidences a good DNA relaxation profile typical for DNA intercalation whereas a strong increase in the upper band (corresponding to open circle plasmid DNA) and a unique intermediate band (that may corresponds to linear DNA form observed by for compound **3d**). Such migration is in agreement with a Topoisomerase I-poisoning effect.

2.5. Topoisomerase I or II poisoning effects

The topoisomerase poisoning effect was confirmed induced migration of the same DNA sample on a ethidium bromide-containing agarose gel in comparison with camptothecin (CPT) that was used as a positive control (Fig. 5). Migration in the presence of BET abolishes the visualization of the topoisomers and relaxed forms which migrate faster, as does supercoiled DNA was well The strong DNA poisoning effect of compounds **3a**, **3b** and **3c** is witnessed by the increase level of the open-circle form. The effect obtained by use of **3a** and **3c** was much stronger in comparison with the control drug CPT, leading to the appearance of an intermediate band corresponding to linear DNA as classically obtained using topoisomerase II (Fig. 6).

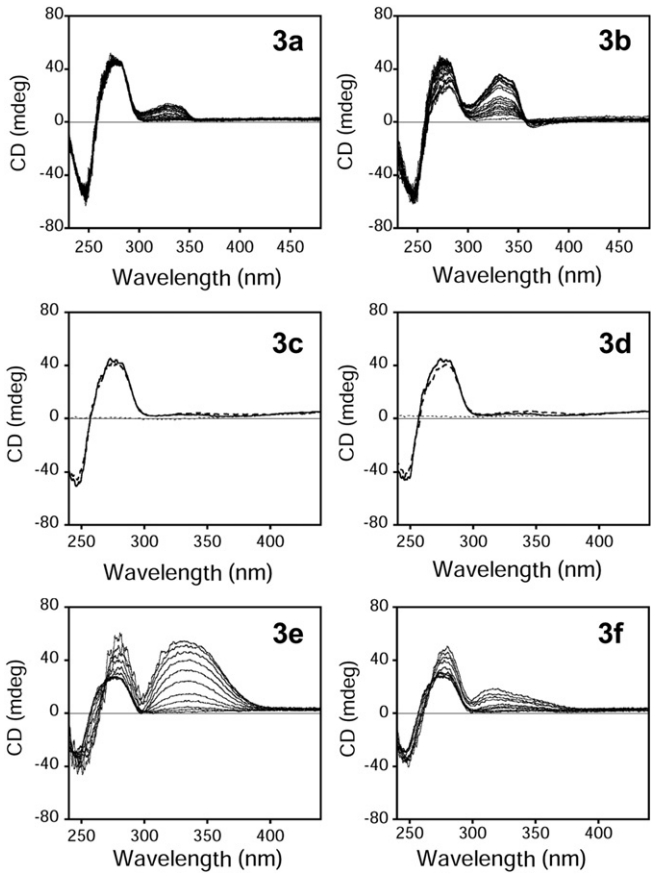

Fig. 2. Circular dichroism spectra. CT-DNA (200 μM) was incubated with increasing concentrations (1, 2, 5, 10, 20, 30, 40, 50, 60 and 80 μM) of **3a**, **3b**, **3e** or **3f** compounds or a fixed concentration (50 μM) of compounds **3c** or **3d** in BPE buffer. Measurements performed using the compound alone evidenced no intrinsic CD of the molecules (data not shown).

The compounds were consequently additionally evaluated for the topoisomerase II poisoning effect (Fig. 6). Used as a reference drug, etoposide evidenced the formation of the linear DNA band. Similar result at a much lesser extent was obtained by use of compounds **3a** and **3c**. Additionally, an increase quantities of the open-circle DNA band suggests partial topoisomerase II cleavage of the DNA leading to single strand cleavage.

3. Conclusion

Novel diamidino substituted conformationally restricted isomeric of bisbenzothiazolyl-phenylenes were efficiently synthesized and converted into the desired water soluble dihydrochloride salts.

Even though all tested compounds showed antiproliferative effects, the strongest activity and cytotoxicity was observed for diimidazolinyl substituted phenylene-bisbenzothiazole **3b** while the highest selectivity towards tumour cells and low cytotoxicity was obtained for compound **3d**. Their antiproliferative activity on tumour cells was concentration-dependant. However, biological mechanisms for these two compounds resulted different according to the tested cell line which is probably dependant on the genetic background of cells. In terms of mechanism of action, several conclusions might be addressed. First, the *meta*- (**3a** and **3b**) and *ortho*- (**3e** and **3f**) substituted compounds present stronger DNA binding propensities than the *para*-substituted ones (**3c** and **3d**) (Table 5). Indeed, induction of apoptosis as a probable consequence of DNA binding ability has been confirmed for diimidazolinyl *meta*-substituted phenylene-bisbenzothiazole compound **3b** on tested cell lines. On the other hand, *para*-substituted compound **3d** induced apoptosis on a weaker extent. In particular, compound **3e** presenting no (or weakest) cytotoxic effect, showed the weakest DNA binding propensity 5.34 (Δ*T*m values), no changes in CD spectra (suggesting no groove binding and no intercalation, as confirmed using topoisomerase I-induced DNA relaxation), no sequence-specific binding (DNase I footprinting, not shown) and no topoisomerase I/II poisoning effects. Second, if the *meta*- (**3a** and **3b**) and *ortho*- (**3e** and **3f**) substituted compounds partially bind in the (minor) groove of the DNA (Fig. 2), only the diimidazolinyl *meta*-substituted phenylene-bisbenzothiazole compound **3b** presents some sequence-selective binding to the DNA at AT-rich sequences (Fig. 3). Interestingly this compound is the most cytotoxic one. It is possible that this sequence-selective binding to the DNA accounts at least partially for observed cytotoxic activity. Third, the diimidazolinyl *para*-substituted compound **3c** and *meta*-substituted compound **3a** presented strong topoisomerase I and II poisoning effects.

In summary, diamidino substituted conformationally restricted isomeric of bisbenzothiazolyl-phenylenes showed strong antiproliferative effects on tested tumour cell lines where the diamidinyl *meta*-substituted phenylene-bisbenzothiazole compound **3b** showed the strongest but non-selective activity on the growth of all tested cell lines, including normal fibroblasts. The major revelation was the diimidazolinyl *para*-substituted phenylene-bisbenzothiazole compound **3d**, which lacks DNA binding abilities. It showed high tumour selectivity and no cytotoxic effect on

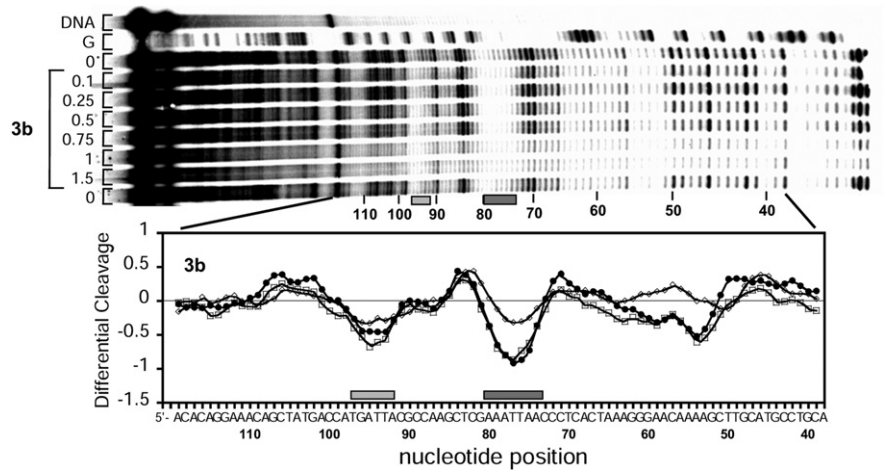

Fig. 3. DNase I footprinting assays. The polyacrylamide gel (top panel) and the corresponding densitometric analysis (bottom panel) of the sequence-selective binding compound **3b** compound was performed on the 3′-end radio-labelled 265 bp DNA fragment. The grey boxes localize the binding sites of the compound along the DNA helix relatively to the base sequence determined from comparison to the G-track lane ("G") used to localize guanines in the DNA fragment and to deduce the migration position of each base within the known sequence. "DNA", DNase-I untreated 265 bp fragment used as quality control.

normal fibroblasts making it an excellent candidate for further chemical optimization and preclinical evaluation.

4. Experimental

4.1. Chemistry

Melting points were determined on a Koffler hot stage microscope. ^{1}H and ^{13}C NMR spectra were recorded on Bruker Avance DPX 300 or Brucker AV-600 spectrometers using TMS, as an internal standard and the deuterated solvents were used, as mentioned. Elemental analysis for carbon, hydrogen and nitrogen were performed on a Perkin–Elmer 2400 elemental analyzer. Analyses are indicated only as symbols of elements, and analytical results obtained are within 0.4% of the theoretical value. Mass spectra were recorded with the Agilent 1100 Series LC/MSD Trap SL spectrometer. Synthesis of 5-amidinium-2-aminobenzothiolate **2a** and 5-(imidazolinium-2-yl)-2-aminobenzothiolate hydrate **2b** were prepared according to the literature [23].

4.1.1. General procedure for preparation of compounds *3a–3d*

To a stirred solution of 5-amidinium-2-aminobenzothiolate **2a** (175 mg, 1.1 mmol) or 5-(imidazolinium-2-yl)-2-aminobenzo thiolate hydrate **2b** (232 mg, 1.1 mmol) in glacial acetic acid (10 mL), isophthaloyl dichloride **1a** (101 mg, 0.5 mmol) or terephthaloyl dichloride **1b** (101 mg, 0.5 mmol) in glacial acetic acid (5 mL) was added under nitrogen and refluxed for 3 h. The reaction mixture was cooled and resulting precipitate filtered off, washed with acetone and dried under vacuum over KOH. The crude product was dissolved in water (20 mL) and to the stirred solution concd hydrochloride acid (2 mL) was added. After cooling overnight the resulting solid was filtered off, washed with acetone and dried. The pure dihydrochloride salt was obtained by crystallization as described below.

*4.1.1.1. 2,2′-(Phenylene-1,3-diyl)bis(1,3-benzothiazole-6-carboximida mide) dihydrochloride (**3a**).* Using above general procedure, and crystallization from water/acetone mixture gave pure compound **3a**, 240 mg (86.3%) as colourless solid: mp >300 °C. ^{1}H NMR (300 MHz, DMSO-d_6) (δ ppm): 9.54 (s, 4H, H-amd), 9.34 (s, 4H, H-amd), 8.93 (s, 1H, H–Ph), 8.78 (s, 2H, H–Bt), 8.41–8.36 (m, 4H, 2H–Ph, 2H–Bt), 8.00 (d, 2H, J = 8.6 Hz, H–Bt), 7.87 (t, 1H, J = 7.8 Hz, H–Ph). LC-MS (ESI) m/z: 429.3 [(M + H$^+$) calcd for free base $C_{22}H_{16}N_6S_2$, 428.09]. Analysis calcd for $C_{22}H_{18}Cl_2N_6S_2 \times 3H_2O$ (555.50): C, 47.57; H, 4.35; N, 15.13. Found C, 47.89; H, 4.09; N, 15.10%.

*4.1.1.2. 2,2′-(Phenylene-1,3-diyl)bis[6-(4,5-dihydro-1H-imidazol-2-yl)-1,3-benzothiazole] dihydrochloride (**3b**).* Using above general procedure, and crystallization from water/acetone mixture gave pure compound **3b** 278 mg (91.4%) as colourless solid: mp >300 °C ^{1}H NMR (600 MHz, DMSO-d_6) (δ ppm): 10.79 (s, 4H, H-Amd),

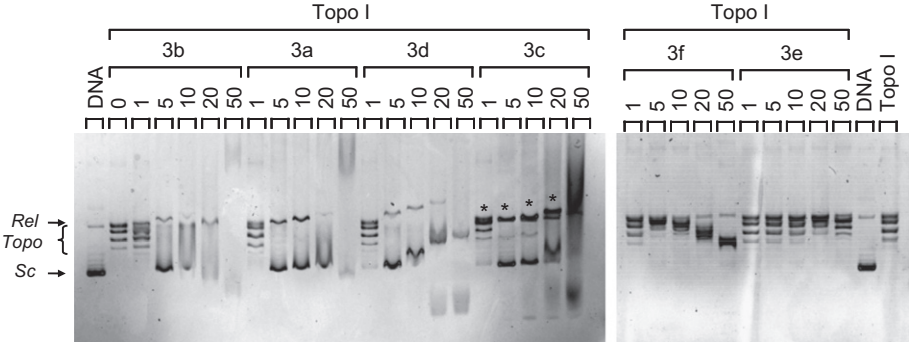

Fig. 4. Topoisomerase I-induced DNA relaxation. Increasing concentrations (μM) of the indicated compounds were incubated with supercoiled (*Sc*) pUC19 plasmid DNA prior to treatment with topoisomerase I enzyme (Topo I) reveal relaxed plasmid (*Rel*), open-circle (*) and various topoisomers (*Topo*). "DNA", untreated supercoiled plasmid DNA.

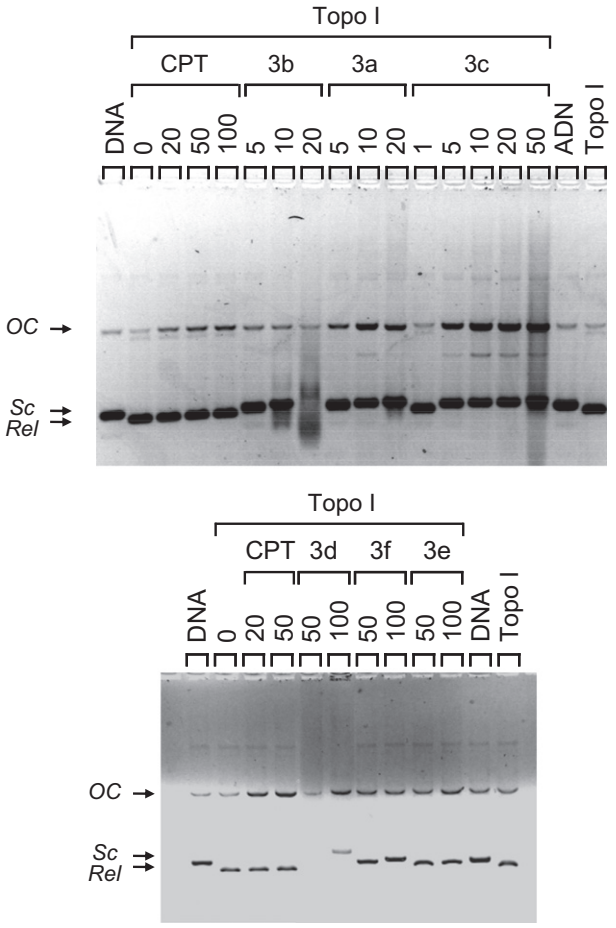

Fig. 5. Topoisomerase I-poisoning effect. The native supercoiled pUC19 plasmid was incubated with topoisomerase I in the absence (lanes Topo I or 0) or presence of compounds **3a** to **3f** or of CPT (used as a reference drug) at the indicated concentrations (μM). The DNA samples were separated using electrophoresis on a 1% agarose gel containing ethidium bromide. *Sc*, *Rel* and *OC* refer to the supercoiled, relaxed and free open circular forms of the plasmid DNA, respectively.

8.94 (s, 1H, H—Ph), 8.90 (d, 2H, J = 1.4 Hz, H—Bt), 8.43—8.40 (m, 4H, 2H—Ph, 2H—Bt), 8.14 (dd, 2H, J = 1.6 Hz, J = 8.6 Hz, H—Bt), 7.89 (t, 1H, J = 7.8 Hz, H—Ph), 4.08 (s, 8H, H—CH_2). ^{13}C NMR (75 MHz, DMSO-d_6/D_2O, 80 °C) (δ ppm): 171.9, 164.5, 156.3, 135.2, 131.8, 131.0, 126.0, 125.0, 123.7, 123.3, 123.1, 118.0, 45.2. LC-MS (ESI) m/z: 481.4

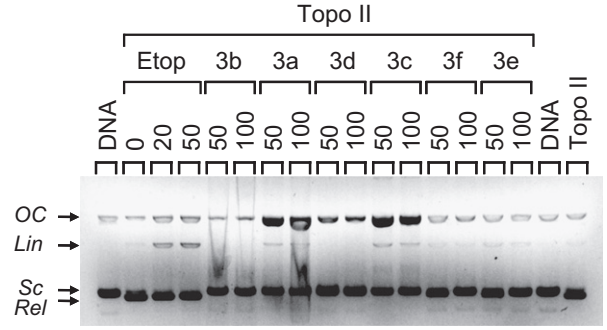

Fig. 6. Topoisomerase II poisoning effect. The various compounds (50 or 100 μM) were incubated with supercoiled pUC19 plasmid DNA ("DNA") prior to treatment with topoisomerase II enzyme ("Topo II"). The DNA samples were separated on an ethidium bromide-containing agarose gel (1%). *Sc*, *Rel*, *OC* and *Lin* refer to the supercoiled, relaxed, free open circular and linear forms of the plasmid DNA, respectively.

[($M + H^+$) calcd for free base $C_{26}H_{20}N_6S_2$, 480.12]. Analysis calcd for $C_{26}H_{22}Cl_2N_6S_2 \times 3H_2O$ (607.57): C, 51.40; H, 4.65; N, 13.83. Found C, 51.18; H, 4.58; N, 13.99%.

*4.1.1.3. 2,2′-(Phenylene-1,4-diyl)bis(1,3-benzothiazole-6-carboximidamide) dihydrochloride (**3c**).* Using above general procedure, and crystallization from water/1 M HCl/acetone mixture gave pure compound **3c**, 251 mg (90.4%) as pale yellow solid: mp >300 °C. ^{1}H NMR (300 MHz, DMSO-d_6) (δ ppm): 9.55 (br s, 4H, H-amd), 9.30 (br s, 4H, H-amd), 8.77 (d, 2H, J = 1.6 Hz, H—Bt), 8.40 (s, 4H, H—Ph), 8.34 (d, 2H, J = 8.5 Hz, H—Bt), 7.99 (dd, 2H, J = 1.8 Hz, J = 8.5 Hz, H—Bt). ^{13}C NMR (75 MHz, D_2O/DMSO-d_6) (δ ppm): 171.9, 164.6, 156.1, 135.2, 134.0, 128.5, 125.7, 123.5, 123.4, 122.5. LC-MS (ESI) m/z: 429.3 [($M + H^+$) calcd for free base $C_{22}H_{16}N_6S_2$, 428.09]. Analysis calcd for $C_{22}H_{18}Cl_2N_6S_2$ x $3H_2O$ (555.50): C, 47.57; H, 4.35; N, 15.13. Found C, 47.63; H, 4.12; N, 15.01%.

*4.1.1.4. 2,2′-(Phenylene-1,4-diyl)bis[6-(4,5-dihydro-1H-imidazol-2-yl)-1,3-benzothiazole] dihydrochloride (**3d**).* Using above general procedure, and crystallization from water/acetone mixture gave pure compound **3d**, 266 mg (87.5%) as pale yellow solid: mp >300 °C. ^{1}H NMR (600 MHz, DMSO-d_6) (δ ppm): 10.62 (s, 4H, H-amd), 8.83 (s, 2H, H-Bt), 8.41—8.38 (m, 6H, 4H—Ph, 2H—Bt), 8.09 (d, 2H, J = 8.6 Hz, H—Bt), 4.08 (s, 8H, H—CH_2). ^{13}C NMR (75 MHz, D_2O/DMSO-d_6) (δ ppm): 172.2, 164.6, 156.6, 135.6, 134.0, 128.2, 126.1, 123.9, 123.3, 118.2, 45.2. LC-MS (ESI) m/z: 481.4 [($M + H^+$) calcd for free base $C_{26}H_{20}N_6S_2$, 480.12]. Analysis calcd for $C_{26}H_{22}Cl_2N_6S_2$ x $3H_2O$ (607.57): C, 51.40; H, 4.65; N, 13.83. Found C, 51.68; H, 4.49; N, 13.80%.

*4.1.2. General procedure for preparation of compounds **3e** and **3f***

To a stirred solution of phthalic acid **1c** (82 mg, 0.5 mmol) in polyphosphoric acid (15 g) dissolved at 120 °C under nitrogen 5-amidinium-2-aminobenzothiolate **2a** (175 mg, 1.1 mmol) or 5-(imidazolinium-2-yl)-2-aminobenzothiolate hydrate **2b** (232 mg, 1.1 mmol) was added. The mixture was heated at 120—140 °C under nitrogen, until it becomes homogeneous (1 h) and then for additional 2 h at 160—180 °C. The reaction mixture was cooled and water (100 mL) was added. The resulting precipitate was filtered off, washed with water and dried. The crude product was suspended in water (50 mL) and made alkaline with 2.5 M NaOH (10 mL). The corresponding free base was filtered off, washed with water and dried under vacuum. The free base was converted into dihydrochloride salt and purified by crystallization from appropriate solvents as described below.

*4.1.2.1. 2,2′-(Phenylene-1,2-diyl)bis(1,3-benzothiazole-6-carboximidamide) dihydrochloride (**3e**).* To a solution of the free base prepared using above general procedure in ethanol (20 mL) concd HCl (0.5 mL) was added and stirred for 1 h. The reaction mixture was concentrated to 5 mL by rotavapor and diethyl-ether (25 mL) was added to give pure compound **3e** 171 mg (61.6%) as colourless solid: mp = 236—238 °C. ^{1}H NMR (300 MHz, DMSO-d_6) (δ ppm): 9.40 (br s, 8H, H-Amd), 8.64 (s, 2H, H—Bt), 8.15 (d, 2H, J = 8.5 Hz, H-Bt), 8.04 (m, 2H, H—Ph), 7.92—7.85 (m, 4H, 2H—Ph, 2H—Bt). ^{13}C NMR (75 MHz, D_2O/DMSO-d_6) (δ ppm): 171.9, 165.9, 155.5, 136.3, 132.0, 131.7, 131.6, 126.2, 125.1, 123.4, 122.9. LC-MS (ESI) m/z: 429.3 [($M + H^+$) calcd for free base $C_{22}H_{16}N_6S_2$, 428.09]. Analysis calcd for $C_{22}H_{18}Cl_2N_6S_2$ x $3H_2O$ (555.50): C, 47.57; H, 4.35; N, 15.13. Found C, 47.81; H, 4.23; N, 15.28%.

*4.1.2.2. 2,2′-(Phenylene-1,2-diyl)bis[6-(4,5-dihydro-1H-imidazol-2-yl)-1,3-benzothiazole] dihydrochloride (**3f**).* To a solution of the free base prepared using above general procedure in ethanol (20 mL) concd HCl (0.5 mL) was added and stirred for 1 h. The reaction

mixture was concentrated to 5 mL by rotavapor and diethyl-ether (60 mL) was added to give pure compound **3f** 206 mg (67.8%) as colourless solid: mp = 238–239 °C. ^{1}H NMR (600 MHz, DMSO-d_6) (δ ppm): 10.95 (s, 4H, H-amd), 8.88 (s, 2H, H–Bt), 8.16 (d, 2H, J = 8.6 Hz, H–Bt), 8.13 (d, 2H, J = 8.6 Hz, H–Bt), 8.07 (m, 2H, H–Ph), 7.87 (m, 2H, H–Ph), 4.02 (s, 8H, H-CH_2). ^{13}C NMR (75 MHz, D_2O) (δ ppm): 171.7, 165.0, 155.3, 136.1, 131.7, 131.3, 131.1, 125.9, 123.2, 122.8, 118.8, 44.6. LC-MS (ESI) m/z: 481.4 [($M + H^+$) calcd for free base $C_{26}H_{20}N_6S_2$, 480.12]. Analysis calcd for $C_{26}H_{22}Cl_2N_6S_2$ x $3H_2O$ (607.57): C, 51.40; H, 4.65; N, 13.83. Found C, 51.73; H, 4.84; N, 13.91%.

4.2. Biological tests

4.2.1. Cell culturing

HeLa (cervical carcinoma), SW620 (colorectal adenocarcinoma, metastatic), MiaPaCa-2 (pancreatic carcinoma), MCF-7 (breast epithelial adenocarcinoma, metastatic), SK-BR-3 (breast adenocarcinoma) and WI38 (normal diploid human fibroblasts) cell lines were cultured as monolayers and maintained in Dulbecco's modified Eagle medium (DMEM) supplemented with 10% fetal bovine serum (FBS), 2 mM L-glutamine, 100 U/ml penicillin and 100 μg/ml streptomycin in a humidified atmosphere with 5% CO_2 at 37 °C.

4.2.2. Proliferation assay

For the antiproliferative assays, cells were inoculated onto a series of standard 96-well microtiter plates on day 0, at 3000–5000 cells per well according to the doubling times of specific cell line. Tested compounds were added in five 10-fold dilutions (0.01–100 μM) and incubated for further 72 h. Working dilutions were freshly prepared on the day of testing in the growth medium. The solvent (DMSO) was also tested for eventual inhibitory activity by adjusting its concentration to be the same as in the working concentrations (DMSO concentration never exceeded 0.1%). After 72 h of incubation, the cell growth rate was evaluated by performing the MTT assay: experimentally determined absorbance values were transformed into a cell percentage growth (PG) using the formulas proposed by NIH and described previously [27]. This method directly relies on control cells behaving normally at the day of assay because it compares the growth of treated cells with the growth of untreated cells in control wells on the same plate – the results are therefore a percentile difference from the calculated expected value.

The IC_{50} and LC_{50} values for each compound were calculated from dose–response curves using linear regression analysis by fitting the mean test concentrations that give PG values above and below the reference value. If, however, all of the tested concentrations produce PGs exceeding the respective reference level of effect (e.g. PG value of 50) for a given cell line, the highest tested concentration is assigned as the default value (in the screening data report that default value is preceded by a "$>$" sign). Each test point was performed in quadruplicate in three individual experiments. The results were statistically analyzed (ANOVA, Tukey post-hoc test at $p < 0.05$). Finally, the effects of the tested substances were evaluated by plotting the mean percentage growth for each cell type in comparison to control on dose response graphs.

4.2.3. Cell cycle analysis

A total of 50,000 cells were seeded per Petri dish (10 cm in diameter, Sarstedt, Germany). After 24 h, MiaPaCa-2, SK-BR-3 and HeLa cells were treated with compounds **3b** and **3d** at concentrations of 5 and 10 μM. SW60 cells were treated only with compound **3b** at same concentrations. After 24 and 48 h, the attached cells were trypsinized, combined with floating cells, washed with PBS, and fixed with 70% ethanol. Immediately before the analysis, the cells were washed again with PBS and stained with 1 μg/mL of propidium iodide (PI) with the addition of 0.2 μg/mL of RNase A. The stained cells were then analysed with Becton Dickinson FACScalibur flow cytometer (10 000 counts were measured). Each test point was performed in duplicate. The percentage of the cells in each cell cycle phase was based on the obtained DNA histograms and determined by using the WinMDI 2.9 and Cylchred software. Statistical analysis was performed in Microsoft Excel by using the ANOVA at $p < 0.05$.

4.2.4. Detection of apoptosis

Annexin V-Fluos staining kit (Roche) assay was used to assess apoptosis induction according to the manufacturer's recommendations. The SW620, SK-BR-3 and MiPaCa-2 cells were seeded on chamber slides (4000 cells/well, Lab-Tk II Chamber slide, Nunc, SAD). SW620 and SK-BR-3 cells were treated with compound **3b** while MiaPaCa-2 and SKBR-3 were treated with compound **3d**. Both compounds were used at concentration of 10 μM for 24 h. Upon treatment, the growth medium was removed from wells. Attached cells were covered with 100 μL/well of incubation buffer, containing Annexin V-Fluos labelling reagent and propidium iodide (PI) 15 min. The cells were then washed with PBS and analysed under the fluorescent microscope. The results are presented as percentages of cells positive to annexin and propidium iodide per total cell number. At least 100 cells were counted in each well.

4.3. DNA binding studies

4.3.1. UV/visible spectrometry and DNA melting temperature studies

For UV/visible spectroscopy, 20 μM of the various compounds were incubated with CT-DNA (Sigma–Aldrich) at increasing concentrations (0.1, 0.2, 0.6, 1, 2, 4, 6, 8, 10, 20, 40, 50, 60, 80, 100 μM) in 1 mL of BPE buffer (6 mM Na_2HPO_4, 2 mM NaH_2PO_4, 1 mM EDTA, pH 7.1), transferred into a quartz cuvette of 10 mm path length and the UV/Visible spectra were recorded from 230 nm to 530 nm using an Uvikon XL spectrophotometer.

For DNA melting temperature studies, 20 μM of CT-DNA was incubated with the various compounds at the drug/DNA ratio of 0.25 or 0.5, optimized for each compound. The DNA absorbency was measured at 260 nm in quartz cells using an Uvikon 943 spectrophotometer thermostated with a Neslab RTE111 cryostat with one measure performed every min over a range of 20–100 °C with an increment of 1 °C per min. The Tm values were deduced from the midpoint of the hyperchromic transition obtained from first-derivative plots. The variation of melting temperature (ΔTm) were calculated by subtracting the Tm values for CT-DNA to that obtained with CT-DNA incubated with the various tested compounds at the indicated drug/base pair ratio.

4.3.2. Circular dichroism

The various tested drugs (50 μM) were incubated with or without (control) a fixed or increasing concentrations of CT-DNA in BPE buffer as previously published [28]. The CD spectra were collected in a 10 mm path length quartz cell cuvette from 430 to 230 nm with a resolution of 0.1 nm using a J-810 Jasco spectropolarimeter fixed at 20 °C by a PTC-424S/L peltier type cell changer (Jasco).

4.3.3. Topoisomerase I-mediated DNA relaxation

This experiment was performed essentially as previously described [29] with the following modifications. The graded concentrations of compounds were incubated with supercoiled pUC19 plasmid DNA before the addition of human topoisomerase I (4U, Topogen, USA) and incubation in relaxation buffer for 45 min at

37 °C. SDS (0.25%) and proteinase K (250 μg/mL) treatment for a 30 min at 50 °C stopped the reaction and removed the protein. The different DNA forms were revealed upon electrophoretic migration on a 1% agarose gel in TBE buffer. The gels were post-stained in a bath containing ethidium bromide, washed and photographed under UV light (GelDoc, BioRad).

4.3.4. Topoisomerases cleavage assays

For topoisomerase I DNA cleavage assays, the samples were prepared as described in the Topoisomerase I-mediated DNA relaxation section above except that the samples were loaded on a 1% agarose gel prepared containing ethidium bromide. Camptothecin was used as a control for topoisomerase I poisoning effect.

Topoisomerase II DNA cleavage assays were performed essentially as described in Ref. [30]. Briefly, supercoiled pUC19 plasmid DNA (350 ng) was incubated with 50 μM of the various compounds or etoposide used as a positive control (20 or 50 μM) prior to the addition of 10 units of human topoisomerase II (TopoGen). After a 45 min incubation at 37 °C for in cleavage buffer, SDS (0.25%) and proteinase K (250 mg/mL) were added for 30 min at 50 °C to stop the reaction. The DNA samples were then loaded on a 1% agarose gel containing ethidium bromide and separated for 2 h at 120 V in TBE buffer. The gels were washed and photographed under UV light (GelDoc, BioRad).

4.3.5. DNase I footprinting assay

The 265 bp *Eco*RI and *Pvu*II DNA fragment was prepared as previously described [31] from double digestion of the pBluscript plasmid (Stratagene, La Jolla, CA) and 3′-end labelling using α-[^{32}P]-dATP (3000 C_i/mmol, PerkinElmer, France). The DNase I footprinting experiments were performed essentially as previously described [32]. The various compounds were incubated with the 265-bp radio-labelled DNA fragment for 15 min at 37 °C to ensure equilibrium prior to DNA digestion upon addition of DNase I in digestion buffer (20 mM NaCl, 2 mM $MgCl_2$, 2 mM $MnCl_2$, pH 7.3). The DNA cleavage products were separated on an 8% denaturing polyacrylamide gel. After migration, gels were soaked in 10% acetic acid, dried under vacuum on a Whatman 3 MM paper to then be exposed on storage screen and analyzed using a Molecular Dynamics STORM 860. Each base was localized from comparison with guanine positions (G-track) classically obtained by dimethyl-sulphate (DMS)/piperidine treatment of the DNA fragment.

Acknowledgements

We greatly appreciate the financial help of the Croatian Ministry of Science Education and Sports (Projects: 1170000000-3283, 335-0000000-3532, 335-0982464-239, 0982464-1356). M.-H. David-Cordonnier thanks the Ligue Nationale Contre le Cancer (Comité du Nord, Septentrion), the Association Laurette Fugain, the Association pour la Recherche sur le Cancer and the Institut pour la Recherche sur le Cancer de Lille (IRCL) for grants, and is grateful to the CHRU de Lille, the Région Nord/Pas-de-Calais and the IRCL for a PhD fellowship to Raja Nhili and the IRCL for technical expertise (Sabine Depauw).

Appendix A. Supplementary data

Supplementary data related to this article can be found at http://dx.doi.org/10.1016/j.ejmech.2013.02.026.

References

[1] P. Diana, A. Martorana, P. Barraja, A. Montalbano, G. Dattolo, G. Cirrincione, F. Dall'Acqua, A. Salvador, D. Vedaldi, G. Basso, G. Viola, Indolo[2,1-a]quinoxaline derivatives, novel potent antitumor agents with dual inhibition of tubulin polymerisation and topoisomerase I, J. Med. Chem. 51 (2008) 2387–2399.
[2] L. Wilson, M.A. Jordan, Microtubule dynamics: taking aim at a moving target, Chem. Biol. 2 (1995) 569–577.
[3] R.M. Kumbhare, K.V. Kumar, M.J. Ramaiah, T. Dadmal, S.N.C.V.L. Pushpavalli, D. Mukhopadhyay, B. Divya, T.A. Devi, U. Kosurkar, M. Pal-Bhadra, Synthesis and biological evaluation of novel Mannich bases of 2-arylimidazo[2,1-b] benzothiazoles as potential anticancer agents, Eur. J. Med. Chem. 46 (2011) 4258–4266.
[4] I. Yldiz-Oren, I. Yalcin, E. Aki-Sener, N. Ucarturk, Synthesis and structure activity relationship of new antimicrobial active multisubstituted benzole derivatives, Eur. J. Med. Chem. 39 (2004) 291–298.
[5] A. Rana, N. Siddiqui, S.A. Khan, Benzothiazoles: a new profile of biological activities, Indian J. Pharm. Sci. 69 (2007) 10–17.
[6] M. Palkar, M. Noolvi, R. Sankangoud, V. Maddi, A. Gaddad, L.V.G. Nargund, Synthesis and antibacterial, activity of a novel series of 2,3-diaryl substituted-imidazo[2,1-b]benzothiazole derivatives, Arch. Pharm. 343 (2010) 353–359.
[7] M. Yoshida, I. Hayakawa, N. Hayashi, T. Agatsuma, Y. Oda, F. Tanzawa, S. Iwasaki, K. Koyama, H. Furukawa, S. Kurakata, Synthesis and biological evaluation of benzothiazole derivatives as potent antitumour agents, Bioorg. Med. Chem. Lett. 15 (2005) 3328–3332.
[8] M.C.E. McFadyen, W.T. Melvin, G.I. Murray, Cytochrome P450 enzymes and tumor therapy-response, Mol. Cancer Ther. 3 (2004) 1503–1504.
[9] I. Ćaleta, M. Kralj, B. Bertoša, S. Tomić, G. Pavlović, K. Pavelić, G. Karminski-Zamola, Novel cyano and amidinobenzothiazole derivatives: synthesis, antitumour evaluationand X-ray quantitative structure-activity relationship (QSAR) analysis, J. Med. Chem. 52 (2009) 1744–1756.
[10] C.R. Gardner, B.B. Cheung, J. Koach, D.S. Black, G.M. Marshall, N. Kumar, synthesis of retinoid enhancers based on 2-aminobenzothiazoles for anticancer therapy, Bioorg. Med. Chem. 20 (2012) 6877–6884.
[11] G. Manfroni, F. Meschini, M.L. Barreca, P. Leyssen, A. Samuele, N. Iraci, S. Sabatini, S. Massari, G. Maga, J. Neyts, V. Cecchetti, Pyridobenzothiazole derivatives as new chemotype targeting the HCV NS5B polymerase, Bioorg. Med. Chem. 20 (2012) 866–876.
[12] K. Li, J.K. Frankowski, C.A. Belon, B. Neuenswander, J. Ndjomou, A.M. Hanson, M.A. Shanahan, F.J. Schoenen, B.S.J. Blagg, J. Aubé, D.N. Frick, Optimization of potent hepatitis C virus NS3 helicase inhibitors isolated from the yellow dyes thioflavine S and primuline, J. Med. Chem. 55 (2012) 3319–3330.
[13] Y.A. Al-Soud, H.H. Al Sa'doni, S.O.W. Saber, R.H.M. Al Shaneek, N.A. Masoudi, R. Loddo, P. La Colla, Synthesis *in vitro* antiproliferative and anti-HIV activity of new derivatives of 2-piperazino-1,3-benzo[d]thiazoles, J. Chem. Sci. 65 (2010) 1372–1380.
[14] J. Das, R.V. Moquin, J. Lin, C. Liu, A.M. Doweyko, H.F. DeFex, Q.S. Fang Pang, S. Pitt, D.R. Shen, G.L. Schieven, J.C. Barrish, J. Wityak, Discovery of 2-amino-heteroaryl- benzothiazole-6-anilides as potent p56 inhibitors, Bioorg. Med. Chem. Lett. 13 (2003) 2587–2590.
[15] A.A. Weekes, A.D. Westwell, 2-Arylbenzothiazole as a privileged scaffolds in drug discovery, Curr. Med. Chem. (2009) 2430–2440.
[16] S. Tasler, O.M. üller, T. Wieber, T. Herz, R. Krauss, F. Totzke, M.H.G. Kubbutat, C. Schächtele, *N*-substituted 2′-(aminoaryl)benzothiazoles as kinase inhibitors: hit identification and scaffold hopping, Bioorg. Med. Chem. Lett. 19 (2009) 1349–1356.
[17] J.B. Chaires, J. Ren, D. Hamelberg, A. Kumar, V. Pandya, D.W. Boykin, W.D. Wilson, Structural selectivity of aromatic diamidines, J. Med. Chem. 47 (2004) 5729–5742.
[18] X. Cai, P.J. Gray Jr., D.D. Von Hoff, DNA minor groove binders: back in the groove, Cancer Treat. Rev. 35 (2009) 437–450.
[19] L. Racané, M. Kralj, L. Šuman, R. Stojković, V. Tralić-Kulenović, G. Karminski-Zamola, Novel amidino substituted 2-phenylbenzothiazoles: synthesis, antitumor evaluation *in vitro* and acute toxicity testing in vivo, Bioorg. Med. Chem. 18 (2010) 1038–1044.
[20] L. Racanè, V. Tralić-Kulenović, R.P. Kitson, G. Karminski-Zamola, Synthesis and "in vitro" antiproliferative activity of new cyano and amidino substituted 2-Phenyl-benzothiazoles, Monatsh. Chem. 137 (2006) 1571–1577.
[21] L. Racanè, R. Stojković, V. Tralić-Kulenović, G. Karminski-Zamola, Synthesis and antitumor evaluation of novel derivatives of 6-Amino-2-phenylbenzo thiazoles, Molecules 11 (2006) 325–333.
[22] L. Racané, V. Tralić-Kulenović, S. Kraljević Pavelić, I. Ratkaj, P. Peixoto, R. Nhili, S. Depauw, M.P. Hildebrand, M.H. David-Cordonnier, K. Pavelić, G. Karminski-Zamola, Novel diamidino-substituted derivatives of phenyl-benzothiazolyl- and dibenzothiazolyl-furans and thiophenes: synthesis, antiproliferative and DNA binding properties, J. Med. Chem. 53 (2010) 2418–2432.
[23] L. Racané, V. Tralić-Kulenović, Z. Mihalić, G. Pavlović, G. Karminski-Zamola, Synthesis of new amidino-substituted 2-aminothiophenoles: mild basic ring opening of benzothiazole, Tetrahedron 64 (2008) 11594–11602.
[24] L. Racané, S. Kraljević Pavelić, I. Ratkaj, V. Stepanić, K. Pavelić, V. Tralić-Kulenović, G. Karminski-Zamola, Synthesis and antiproliferative evaluation of some new amidino- substituted bis-benzothiazolyl-Pyridines and Pyrimidine, Eur. J. Med. Chem. 55 (2012) 108–116.
[25] T.D. Bradshaw, M.C. Bibby, J.A. Double, I. Fichtner, P.A. Cooper, M.C. Alley, S. Donohue, S.F. Stinson, J.E. Tomaszewjski, E.A. Sausville, M.F.G. Stevens,

Preclinical evaluation of amino acid prodrugs of novel antitumour 2-(4-amino-3-methylphenyl)benzothiazoles, Mol. Cancer Ther. 1 (2002) 239–246.
[26] T.D. Bradshaw, M.S. Chua, H.L. Browne, V. Trapani, E.A. Sausville, M.F.G. Stevens, In vitro evaluation of amino acid prodrugs of novel antitumour 2-(4-amino-3-methylphenyl)benzothiazoles, Br. J. Cancer 86 (2002) 1348–1354.
[27] T. Gazivoda, M. Plevnik, J. Plavec, S. Kraljevic, M. Kralj, K. Pavelić, J. Balzarini, E. De Clercq, M. Mintas, S. Raić-Mali&cacute, The novel pyrimidine and purine derivatives of 3-*O*-benzyl-2-hydroxy- and 2,3-dihydroxy-4,5-didehydro-5,6-dideoxy-L-ascorbic acid: synthesis, one- and two-Dimensional ^{1}H and ^{13}C NMR study, cytostatic and antiviral evaluation, Bioorg. Med. Chem. 13 (2005) 131–139.
[28] T. Serbetçi, S. Depauw, S. Prado, F.-X. Porée, M.-P. Hildebrand, M.-H. David-Cordonnier, S. Michel, F. Tillequin, Benzo[c][1,7] and [1,8]phenanthrolines substituted with anaminoalkyl chain: synthesis and evaluation of the cytotoxicity and the topoisomerase 1 inhibition, Eur. J. Med. Chem. 45 (2010) 2547–2558.
[29] P. Peixoto, C. Bailly, M.H. David-Cordonnier, Topoisomerase I-mediated DNA relaxation as a tool to study intercalation of small molecules into supercoiled DNA, Methods Mol. Biol. 613 (2010) 235–256.
[30] M.H. David-Cordonnier, M.-P. Hildebrand, B. Baldeyrou, A. Lansiaux, C. Keuser, K. Benzschawel, T. Lemster, U. Pindur, Design, synthesis and biological evaluation of new oligopyrrole carboxamides linked with tricyclic DNA-intercalators as potential DNA ligands or topoisomerase inhibitors, Eur. J. Med. Chem. 42 (2007) 752–771.
[31] M.H. David-Cordonnier, C. Gajate, O. Olmea, W. Laine, J. de la Iglesia-Vicente, C. Perez, C. Cuevas, G. Otero, C. Bailly, F. Mollinedo, DNA and non-DNA targets in the mechanism of action of the antitumour drug Yondelis™ (trabectedin, ET-743), Chem. Biol. 12 (2005) 1201–1210.
[32] P. Peixoto, Y. Liu, S. Depauw, D.W. Boykin, C. Bailly, W.D. Wilson, M.H. David-Cordonnier, Direct inhibition of the DNA binding activity of POU transcription factors Pit-1 and Brn-3 by selective binding of a phenyl-furan-benzimidazole dication, Nucleic Acids Res. 36 (2008) 3341–3353.